Pattern Formation and Localized Structures in Reaction-Diffusion Systems with Non-Fickian Transport

M. G. Clerc, E. Tirapegui, and M. Trejo

Departamento de Física, Facultad de Ciencias Físicas y Matemáticas, Universidad de Chile, Casilla 487-3, Santiago, Chile
(Received 16 August 2005; published 25 October 2006)

We study the robust dynamical behaviors of reaction-diffusion systems where the transport gives rise to non-Fickian diffusion. A prototype model describing the deposition of molecules in a surface is used to show the generic appearance of Turing structures which can coexist with homogeneous states giving rise to localized structures through the pinning mechanism. The characteristic lengths of these structures are in the nanometer region in agreement with recent experimental observations.

Reaction-diffusion systems have played an important role in the study of generic spatiotemporal behavior of far from equilibrium systems. These models apply to situations in which one has to describe an extended system in which one can imagine the occupied physical space to be divided in small cells, which are macroscopic in the sense that the relevant macroscopic (intensive) variables vary slowly in each cell and in which we are interested in the study of spatial inhomogeneities with typical lengths bigger than the linear dimensions of the individual cells. We can then consider that this mesoscopic modelization [1] should include two essential features: the local dynamics of the variables inside each cell and the transport phenomena between the cells. We can think of chemical reactions: the variables will be the concentrations of the chemical species involved, the local dynamics will be determined by the chemical reactions inside each cell, which we can model as birth and death processes, and the transport will be the diffusion of these species between the cells which we can model as some kind of random walk in space. In this way we can construct a stochastic description (see, for example, [2]) since fluctuations are being considered, and the macroscopic evolution models will be the equations for the mean values of our variables in the limit of vanishing fluctuations. In the most standard reaction-diffusion models one modelizes transport as normal symmetric random walk with transitions to the $2d$ neighboring cells (d is the spatial dimension) and this will lead a Fickian diffusion term in the macroscopic deterministic models. The robust dynamical behaviors of these standard reaction-diffusion models have been extensively studied [3] including the appearance of spatial patterns first pointed out by Turing [3].

We shall study here robust behaviors of reaction-diffusion models which apply to situations in which transport cannot be described by Fickian diffusion. The non-Fickian character can arise from potential interaction between the *particles* (which will be, for example, the molecules which take part in a chemical reaction), by allowing only a finite occupancy of each cell, or any other mechanism modifying the normal unconstrained random walk

between cells. We shall see that rich complex dynamics arise in a direct way in this case, in particular, we can see the appearance of natural intrinsic lengths depending on the parameters (and not in the geometry) which play an essential role in pattern formation, front dynamics, and in the existence of localized structures. These facts are obviously a consequence of the non-Fickian diffusion and we do not need here strong differences in the diffusion constants to form patterns.

The typical deterministic equations which will interest us are then of the form $\partial_t c(\vec{r}, t) = R[c(\vec{r}, t)] - \vec{\nabla} \cdot \vec{J}[c(\vec{r}, t)]$, where $c(\vec{r}, t)$ stands collectively for the variables, $R[c(\vec{r}, t)]$ for the local dynamics inside each cell (for example, the reaction terms of the chemical reactions), and $\vec{J}[c(\vec{r}, t)]$ is a flux which represents the transport terms (which in the standard case leads to Fickian diffusion). We shall consider in what follows a prototype model of this kind of situation which has been proposed to describe the deposition of a monolayer of molecules in a surface where they can move or react. The equations are (see Ref. [4])

$$\partial_t c(\vec{r}, t) = R[c(\vec{r}, t)]$$
$$+ \vec{\nabla} \cdot \left[D\vec{\nabla} c(\vec{r}, t) - \frac{D}{k_B T} c(1 - c) \vec{\nabla} U(\vec{r}) \right], \quad (1)$$

where the field $c(\vec{r}, t)$, the local coverage, is defined as the quotient between the number of adsorbed molecules in a cell of the surface and the fixed number of available sites in each cell ($c(\vec{r}, t) \leq 1$). The term $D\nabla^2 c$ in (1) is normal diffusion with coefficient D, k_B is Boltzmann constant, T the temperature, and the last term represents the flow of the adsorbed molecules which move under the force given by the gradient of the potential $U(\vec{r})$ produced in that point by the other molecules. The factor $(1 - c)$ takes care of the fact that the flow can only pass through the available vacant sites in each cell (*a finite occupancy effect*) and the potential can be written as $U(\vec{r}) = - \int u(\vec{r} - \vec{r}') c(\vec{r}') d\vec{r}'$ where the function $u(\vec{r})$ is a spherically symmetric interaction potential between molecules separated by a distance $|\vec{r}|$. When the interaction radius is small compared to the diffusion length and the covering $c(\vec{r}, t)$ does not vary

significantly within the interaction radius, we can approximate the integral by $\varepsilon_0 c(\vec{r}) + \zeta_0^2 \nabla^2 c(\vec{r})$ with $\varepsilon_0 = \int u(\vec{r})d\vec{r}$, $\zeta_0^2 = \frac{1}{2}\int|\vec{r}|^2 u(\vec{r})d\vec{r}$, and we have used $\int \vec{r}u(\vec{r})d\vec{r} = 0$ due to symmetry.

The flux $\vec{J}[c(\vec{r}, t)]$ in Eq. (1) is proportional to the conjugate thermodynamic force which arises from the spatial variation of the associated chemical potential $\varphi[c(\vec{r}, t)]$, , i.e., $\vec{J}[c(\vec{r}, t)] = -M(c)\vec{\nabla}\varphi[c(\vec{r}, t)]$, where $M(c) = Dc(1 - c)/k_B T$ is the mobility and φ will be the functional derivative of a *free energy*, $\varphi[c(\vec{r}, t)] = \delta\mathcal{F}[c(\vec{r})]/\delta c(\vec{r})$. Equation (1) can be written in the form $\partial_t c(\vec{r}, t) = R[c(\vec{r}, t)] + \vec{\nabla}\cdot[Mc(\vec{r}, t)\vec{\nabla}\frac{\delta\mathcal{F}[c(\vec{r})]}{\delta c(\vec{r})}]$, with $\mathcal{F}[c, \vec{\nabla}c] = \int_s [k_B T f(c) - \varepsilon_0 c^2/2 + \zeta_0^2|\vec{\nabla}c|^2/2]dr$, with $f(c) = (1 - c)\ln(1 - c) + c\ln(c)$.

The reaction rate has the expression $R[c] = k_{\text{ad}}Ps(1 - c) - k_{\text{des}}c^n$, where P is the pressure of the gas above the adsorbed layer, s is the sticking coefficient, k_{ad} and k_{des} are the adsorption and desorption constant rates, respectively, and $n = \{1, 2\}$. This parameter gives account of the type of activated desorption processes considered: linear ($n = 1$) or nonlinear ($n = 2$). The adsorption and desorption rates are functions of the physical parameters involved in the deposition mechanism and according to the processing method, they may also depend on the coverage field $c(\vec{r}, t)$ [4]. However, for processing methods such as sputtering and laser assisted deposition (nonequilibrium processes), in some temperature range the assumption of constant desorption rate independent of the coverage is fully justified [5]. We shall further simplify our model taking a constant mobility $M(c) = M$ independent of $c(\vec{r}, t)$; this will not change the qualitative dynamics of the model which is our interest here. The equations are then

$$\partial_t c = k_{\text{ad}}Ps(1 - c) - k_{\text{des}}c^n + M\vec{\nabla}^2\varphi,$$
$$\varphi = -\varepsilon_0 c + k_B T \ln\left[\frac{c}{1 - c}\right] - \zeta_0^2\vec{\nabla}^2 c. \quad (2)$$

We recall that stationary state and their linear stability have been studied in a similar model with constant or exponential dependence of desorption rate, for $n = 1$ [6–8], and for $n = 2$ [5].

In the case of linear desorption ($n = 1$), the above model only exhibits one uniform coverage state $c_0 = \kappa/(1 + \kappa)$, $\kappa \equiv k_{\text{ad}}Ps/K_{\text{des}}$, and for nonlinear desorption ($n = 2$), the system has two uniform coverage states, only one with physical sense $c_0 = (-\kappa + \sqrt{\kappa^2 + 4\kappa})/2$ ($0 \leq c_0 \leq 1$). For the linear desorption, the uniform state c_0 exhibits a spatial instability for a critical temperature $T_p = 4T_c c_0(1 - c_0)[1 - 2\sqrt{K_{\text{des}}(1 + \kappa)\zeta_0^2/M\varepsilon_0^2}]$ ($T_p < T_c$) and the system shows patterns with sizes lying in the nanometer range [7]. In this reference the bifurcation diagram of pattern formation is determined close to the spatial instability and it is shown that this bifurcation is of the supercritical type, that is, close to the instability appears a pattern with small amplitude (proportional

to the square root of the bifurcation parameter). This picture is modified when we consider nonlinear desorption; the uniform adsorption state c_0 can now exhibit a subcritical spatial bifurcation for $T_p = 4T_c c_0(1 - c_0)[1 - 2\sqrt{K_{\text{des}}\zeta_0^2/M\varepsilon_0^2}\sqrt[4]{\kappa^2 + 4\kappa}]$ and spatial length $\lambda = 2\pi\sqrt[4]{K_{\text{des}}}\sqrt[8]{\kappa^2 + 4\kappa}$, that is, at the onset of the spatial instability, the system exhibits a pattern with large amplitude and hysteresis with the uniform coverage state. In Fig. 1, we show the amplitude A of the steady state observed in the one-dimensional model (2). This bifurcation is characterized by two critical points, the bifurcation point $\mu_p = T/4T_p$ (cf. Fig. 1), and the bistablity point μ_{sn} (point in the parameter space where the pattern state appears by saddle-node bifurcation). Note that in general, it is a thorny task to find μ_{sn} as a function of the physical parameters. Between these two points, the system exhibits a coexistence between the uniform and spatial periodic coverage states (hysteresis). Inside this parameter region, we observe a localized pattern in one and two spatial dimensions. In Fig. 2, we present the typical localized patterns observed in the model (2). One can understand these localized structures as patterns extended only over a small portion of an extended system. From the point of view of dynamical systems theory, the localized patterns in 1-d spatial systems are homoclinic connections of the spatial dynamical system [9,10].

In order to estimate the spatial size of patterns and localized structures, we can consider the typical values of the Al deposited on TiN(100); at room temperature the lattice constant is $a_{\text{Al}} = 4.05 \times 10^{-10}$ m, the pair interaction energy $\varepsilon = -0.22$ eV, the lattice coordination number $\gamma = 4$ ($\varepsilon_0 = \gamma\varepsilon$ and $\zeta_0 = \gamma\varepsilon a^2$), and molecular dynamics simulations give the diffusion coefficient $D = K_B TM = 10^{-10}$ cm^2/s. Hence, the spatial size of patterns and localized structures is of the order of 30 nm, and these localized structures are *nanolocalized patterns*. It is important to notice that experimentally vacancy islands of the order of the nanometer have been observed in an absorbed monoatomic layer of Ag deposited at room temperature on Ru(0001) [11].
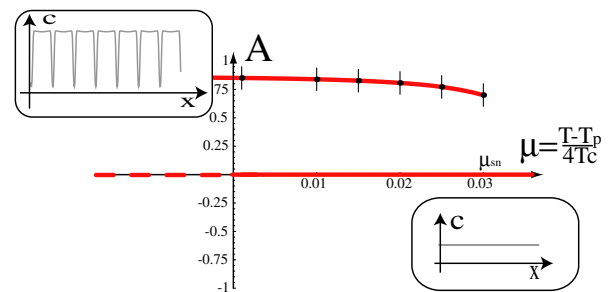
FIG. 1 (color online). Bifurcation diagram of model (2), close to the spatial bifurcation, for: $c_o = 0.8626$, $k_{\text{des}} = 0.0007$, $k_{\text{ad}}Ps = 0.00379$, $n = 2$, and $\Gamma \equiv M\varepsilon_o^2/\zeta_o^2 = 1$. The saddle-node bifurcation of the spatial periodic solution occurs for $\mu_{\text{sn}} = 0.02927$.
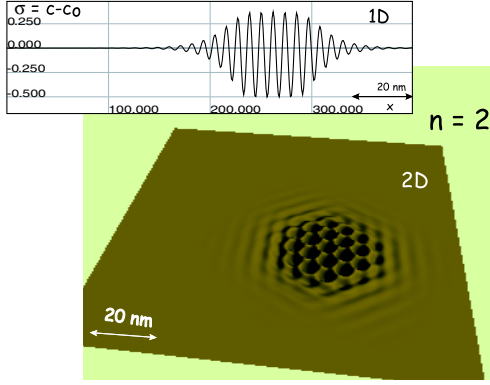
FIG. 2 (color online). Nanolocalized pattern obtained from model (2) for: $\mu = 0.0092$, $C_o = 0.5$, $K_{ad}Ps = 0.008$, $K_{des} = 0.16$, $\Gamma = 1$, and $n = 2$. $\sigma \equiv C - C_o$ and the extreme values are $\sigma_{min} = -0.49916$ and $\sigma_{max} = 0.370704$.

To describe analytically the localized solutions observed in one-dimensional extended systems close to the spatial instability, we use the ansatz $C = C_0 + A(x, t)e^{ik_c x} + \ldots + W$, where A is the amplitude of the spatially oscillatory solution, k_c is the critical wave number ($k_c = 2\pi/\lambda_c$), and W is a small correction function. Introducing the above ansatz in Eq. (2) and linearizing in W, we obtain the following solvability condition

$$\partial_t A = c_1 A + c_3 |A|^2 A + c_5 |A|^4 A + \mathcal{D}\partial_{xx}A + \text{h.o.t.,} \quad (3)$$

where h.o.t stands for the resonant higher order terms and $c_1 = \mu|\varepsilon_0|/2$ is the bifurcation parameter. Hence, when c_1 is positive the system exhibits pattern formation. The parameter c_3 controls the type of the bifurcation (super or subcritical bifurcation depending on the sign of this coefficient, for $c_3 > 0$ the bifurcation is supercritical), $\mathcal{D}$ is the effective diffusion for the amplitude A, and if $c_5 < 0$ and $c_3 \ll 1$, using the scaling $A \sim \sqrt[4]{c_1}$, $\partial_t \sim c_1$, $c_3 \sim \sqrt{c_1}$, $c_5 \sim \mathcal{D} \sim O(1)$, and $\partial_x \sim \sqrt{c_1}$, we can neglect the higher order terms. The full (and lengthy) expressions of these coefficients $\{c_3, c_5, \mathcal{D}\}$, as a function of their physical parameters, are determined by standard normal form techniques [12]. In Fig. 3, we exhibit the values of the coefficients as functions of the uniform coverage stage. In the region of parameters of the subcritical bifurcation (cf. gray region of Fig. 3) the above amplitude equation exhibits coexistence between the uniform state ($A = 0$) and the pattern coverage state ($A = \sqrt{|c_3 + \sqrt{c_3^2 - 4c_1 c_5}|/2|c_5|}$). However, the resonant amplitude equation does not exhibit localized structures because these solutions are a consequence of the interaction of the large scale envelope (A) with the small scale underlying the spatially periodic solution (contained in the nonresonant terms) [13]. To describe the localized structure, we consider the *amended amplitude equation* with the dominant nonresonant terms

$$\partial_t A = c_1 A + c_3 |A|^2 A + c_5 |A|^4 A + \mathcal{D}\partial_{xx}A$$
$$+ (m_1 |A|^2 A^2 + m_2 A^4)e^{ik_c x/\sqrt{c_1}}, \quad (4)$$
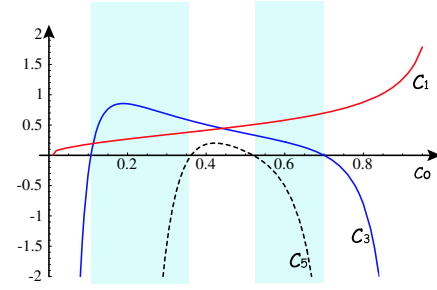
FIG. 3 (color online). Coefficients of the amplitude Eq. (3) as function of the uniform coverage state c_0. The other physical parameters have been fixed to $\Gamma = 1$, $\mu = 0.0092$, and $K_{des} = 0.16$.

where $\{m_1, m_2\}$ are complex and depend on the physical parameters. Notice that the nonresonant terms play the role of a spatial parametric forcing with rapidly varying oscillations and these terms restore the discrete spatial invariance of the amplitude ($x \to x + x_0$, $A \to Ae^{ik_c x_0}$).

The resonant amplitude equation has analytical solutions for a front which links the uniform to the spatially periodic coverage states, and this solution is the starting point to calculate the front interaction. Because of the oscillatory nature of the front interaction, which alternates between attractive and repulsive, we infer the existence, stability properties, dynamical evolution, and bifurcation diagram of localized patterns. These localized structures are a consequence of *the pinning effect*, as it can be seen in an alike amended amplitude equation deduced from a prototype model of pattern formation [13]. Moreover, the existence of these localized structures can be proved rigorously using the tools of dynamical systems theory in the spatial dynamical system [9].

Note that the previous theoretical analysis of patterns and localized patterns is valid for moderate coverage ($0.3 \sim c_0 \sim 0.7$). In the case of low (high) coverage, which is observed for small (large) desorption rate, the spatial bifurcation is supercritical; subsequently we cannot expect nanolocalized structures with small amplitude. However, numerically in one and two dimensions, we observe a pattern with colossal amplitude which coexists with the uniform coverage state of low or high coverage. Hence, in 1D due to the general dynamics system argument [9], we expect the system to exhibit *nanolocalized structures* supported by low or high coverage, that is, the system exhibits a region of full (partial) coverage surrounded by a region of partial (full) coverage. We term these solutions as *absorton* and *vacanton*, respectively. In Figs. 4 and 5, we show these localized nanostructures in one and two spatial dimensions observed for linear and a nonlinear desorption process. In order to explain these localized structures we consider the extreme limit of small reaction terms ($k_{ad}Ps, nk_{des} \ll 1$) where the dynamics around the uniform coverage state can be approached by a perturbed Cahn-Hilliard model [5]

$$\partial_\tau u = \vec{\nabla}^2(\tilde{\varepsilon}u + u^3 - \vec{\nabla}^2 u) + a + bu - cu^n, \quad (5)$$
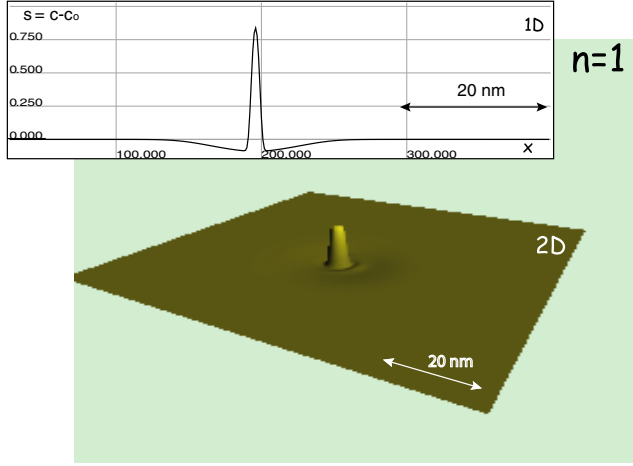
FIG. 4 (color online). Absorton: nanolocalized pattern obtained from model (2) for: $n = 1$, $C_o = 0.9$, $\mu = 0.105$, $K_{ad}Ps = 0.0005$, and $K_{des} = 0.0045$. The extreme values of recover are $\sigma_{min} = -0.0852$, $\sigma_{max} = 0.83814$, and $\sigma \equiv C - C_o$.

where $u(r' = \zeta_0/\sqrt{\varepsilon_0\theta}r, \tau = \Gamma\theta^2 t) = C - C_0 + u_0$, $\tilde{\varepsilon} = [-1 + \mu/C_0(1 - C_0)]/\theta - 3u_0^2$, $a = -(K_{ad}Psu_0 + K_{des}u_0^2)/\Gamma\theta^2$, $b = (K_{ad}Ps + 2K_{des}u_0)/\Gamma\theta^2$, $c = k_{des}/\Gamma\theta^2$, $u_0 \equiv \omega/3\theta$, $\omega \equiv \mu(2C_0 - 1)/2C_0^2(C_0 - 1)^2$, $\theta \equiv -\mu(3C_0^2 - 3C_0 + 1)/3C_0^3(C_0 - 1)^3$, $\Gamma \equiv M\varepsilon_0^2/\zeta_0^2$. $\{a, b, c\}$ are small coefficients. It is well known that the Cahn-Hilliard model exhibits a family of localized solutions (bubbles) [14]. Hence, in the extreme limit, imposing the persistence of the bubble solution we can find analytically the vacanton and absorton solutions which have the expressions $u(x, t) \sim \sqrt{\tilde{\varepsilon}}\tanh[\frac{\sqrt{\tilde{\varepsilon}}}{2}(x + \frac{\Delta}{2})] \mp \sqrt{\tilde{\varepsilon}} - \sqrt{\tilde{\varepsilon}}\tanh[\frac{\sqrt{\tilde{\varepsilon}}}{2} \times (x - \frac{\Delta}{2})]$, where $\Delta = (a - b\sqrt{\tilde{\varepsilon}} + c\tilde{\varepsilon})L/(2b\sqrt{\tilde{\varepsilon}} - c\tilde{\varepsilon})$, and L is the size of the system. The above solution represents a vacanton (absorton) for positive (negative) Δ and sign
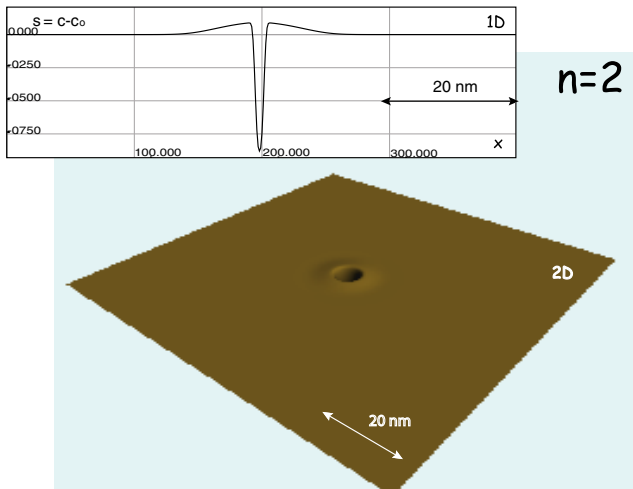
FIG. 5 (color online). Vacanton: nanolocalized pattern obtained from model (2) for: $n = 2$, $C_o = 0.9009$, $K_{ad}Ps = 0.00409$, $K_{des} = 0.0005$, $\Gamma = 1$, and $\mu = 0.1$. The extreme values of coverage are $\sigma_{max} = 0.0087$, $\sigma_{min} = -0.87$, and $\sigma \equiv C - C_o$.

$-$ (+). It is worth to remark that in this extreme limit the localized solutions depend on the size of the system and when $L \rightarrow \infty$ the system does not exhibit nanolocalized structures. In the case of $\{a, b\} \ll c \ll 1$, we observe numerically only vacanton solutions as the analytical result shows. We have checked the variation of the size of the vacanton as function of the system size.

In the case of low (high) coverage and for linear desorption ($n = 1$), the spatial bifurcation is supercritical; subsequently, we cannot expect nanolocalized structures with small amplitude. However, numerically in one and two dimensions, we observe a pattern with colossal amplitude which coexists with the uniform coverage state of low or high coverage. Hence, the system also exhibits nanolocalized structures supported by low or high coverage. In an analogous way from the model (2), we can approach the system by the perturbed Cahn-Hilliard Eq. (5) and obtain a nanolocalized solution, vacanton or absorton, with a size $\Delta = [a - (b - c)\sqrt{\tilde{\varepsilon}}]L/2(b - c)\sqrt{\varepsilon}$. Therefore, the nanolocalized solutions are a robust phenomena in the covering dynamics, when the system has two ingredients: local kinetic processes and non-Fickian transport as stated in the introduction.

[1] N. G. Van Kampen, *Stochastic Process in Physics and Chemistry* (North-Holland, Amsterdam 1992).
[2] F. Langouche, D. Roekaerts, and E. Tirapegui, Phys. Lett. **82A**, 309 (1981).
[3] G. Nicolis and I. Prigogine, *Self-Organization in Non-Equilibrium Systems* (Wiley, New York, 1977).
[4] A. S. Mikhailov and M. Hildebrand, J. Phys. Chem. **100**, 19 059 (1996).
[5] J. Verdasca, G. Dewel, and P. Borckmans, Phys. Rev. E **55**, 4828 (1997).
[6] D. Waelgraf, Philos. Mag. **83**, 3829 (2003).
[7] D. Waelgraf, Physica (Amsterdam) **15E**, 33 (2002).
[8] M. Hildebrand, A. S. Mikhailov, and G. Ertl, Phys. Rev. E **58**, 5483 (1998).
[9] P. Coullet, C. Riera, and C. Tresser, Phys. Rev. Lett. **84**, 3069 (2000).
[10] M. C. Cross and P. C. Hohenberg, Rev. Mod. Phys. **65**, 851 (1993).
[11] K. Pohl, M. C. Bartelt, J. de la Figuera, N. C. Bartelt, J. Hrbek, and R. Q. Hwang, Nature (London) **397**, 238 (1999).
[12] C. Elphick, E. Tirapegui, M. Brachet, P. Coullet, and G. Iooss, Physica (Amsterdam) **29D**, 95 (1987).
[13] M. G. Clerc and C. Falcon, Physica (Amsterdam) **356A**, 48 (2005).
[14] H. Calisto, M. Clerc, R. Rojas, and E. Tirapegui, Phys. Rev. Lett. **85**, 3805 (2000); M. Argentina, M. G. Clerc, R. Rojas, and E. Tirapegui, Phys. Rev. E **71**, 046210 (2005).